Tropical Cyclone Ensemble Data Assimilation

Istvan Szunyogh
Texas A&M University, Department of Atmospheric Sciences, 3150 TAMU, College Station, TX, 77843-3150
phone: (979) 458-0553 fax: (979) 862-4466 email: szunyogh@tamu.edu

Award Number: N000140910589
http://atmo.tamu.edu/profile/ISzunyogh

LONG-TERM GOALS

The ultimate goal of this project is to demonstrate that in the presence of tropical cyclones (TCs), a multi-scale approach for data asssimilation can significantly ehnance the analyses and the ensuing forecasts. Our multiscale approach is based on coupling a lower resolution global data assimilation system and a higher resolution limited area data assimilation system in a TC basin. The coupled approach has the potential to lead to a better utilization of the available atmospheric observations and computer resources.

OBJECTIVES

Ours is the first attempt to use an ensemble-based, coupled global-limited-area data assimilation system to improve the analyses and the forecasts of TCs and their effects on the larger scale atmospheric processes. In fact, to the best of our knowledge, ours has been the only research group working on a data assimilation system that generates both global and limited area analyses. Our key scientific objective is to explore the potentials and the limitations of the coupled global-limited-area data assimilation approach. This research objective is particularly relevant for the numerical weather forecasting applications of the Navy, as the Fleet Numerical Meteorology and Oceanography Center (FNMOC) prepares both a global forecast and a larger number of limited area forecasts (more than 60) than any other forecast center in the world.

APPROACH

Our data assimilation system is based on the Local Ensemble Transform Kalman Filter (LETKF) algorithm (Ott et al. 2004; Hunt et al. 2007) and its specific implementation on the NCEP GFS model (Szunyogh et al. 2005 and 2008). The first effort led by the PI to build a coupled global-limited-area data assimilation system was described in Merkova et al. (2011). That paper compared the performance of four different coupling strategies for an extended North-American region. Based on the experience of that study, we chose a strategy for the assimilation of observations in a TC basin, where an ensemble-based global data assimilation system provides the initial conditions for a global

Report Documentation Page

Form Approved
OMB No. 0704-0188

1. REPORT DATE	2. REPORT TYPE	3. DATES COVERED
2012	**N/A**	**-**

4. TITLE AND SUBTITLE	5a. CONTRACT NUMBER
Tropical Cyclone Ensemble Data Assimilation	5b. GRANT NUMBER
	5c. PROGRAM ELEMENT NUMBER
6. AUTHOR(S)	5d. PROJECT NUMBER
	5e. TASK NUMBER
	5f. WORK UNIT NUMBER
7. PERFORMING ORGANIZATION NAME(S) AND ADDRESS(ES) **Texas A&M University, Department of Atmospheric Sciences, 3150 TAMU, College Station, TX, 77843-3150**	8. PERFORMING ORGANIZATION REPORT NUMBER
9. SPONSORING/MONITORING AGENCY NAME(S) AND ADDRESS(ES)	10. SPONSOR/MONITOR'S ACRONYM(S)
	11. SPONSOR/MONITOR'S REPORT NUMBER(S)

12. DISTRIBUTION/AVAILABILITY STATEMENT
Approved for public release, distribution unlimited

13. SUPPLEMENTARY NOTES
The original document contains color images.

14. ABSTRACT

15. SUBJECT TERMS

16. SECURITY CLASSIFICATION OF:			17. LIMITATION OF ABSTRACT	18. NUMBER OF PAGES	19a. NAME OF RESPONSIBLE PERSON
a. REPORT	b. ABSTRACT	c. THIS PAGE			
unclassified	**unclassified**	**unclassified**	**SAR**	**17**	

ensemble, which then provides the ensemble of lateral boundary conditions for the limited area data assimilation system. We configured the limited area system for the West Pacific Typhoon basin. Experiments were carried out for the 2004 and 2008 typhoon seasons.

WORK COMPLETED

In the third (final) year of the project we focused on four closely related research isssues:

1. Final refinement of the results for the 2004 Typhoon season. These results were summarized in the paper Holt et al. (2012), which was submitted for publication in early 2012. The paper received favorable reviews and was revised to address the referees' comments. The revised version has been submitted and we are waiting for the editor's decision.
2. A reanalysis of observations collected during the 2008 Typhoon season (TCS-08 field program). We are in the process of preparing a paper for submission based on these results.
3. The assimilation of QuikSCAT observations of Typhoon Mindulle (2004). We worked on this component of the project in close collaboration with our collaborators from AER Inc.
4. The PI continued his close collaboration with scientists from the University of Maryland on further developing the theory of the joint state approach for coupled global-limited-area data assimilation. The most important results of that research are summarized in the paper Yoon et al. (2012), which has been accepted for publication and is currently in press.

In what follows, we summarize the most important results for each of the above research topics.

RESULTS

New Results for the 2004 Typhoon Season

The resolution of global analysis/forecast system was T62 (about 240 km in the West Pacific typhoon basin), while the resolution of the limited area system varied between 200 km, 100 km, 48 km and 36 km. As was reported earlier, the limited area data assimilation system clearly enhanced the analyses compared to the global analyses, but increasing the resolution beyond 100 km had little benefit in terms of the accuracy of the position analysis. In the third year of the project we focused on developing an understanding of this finding.

First, we investigated the changes in the quality of the analysis of the steering flow due to the addition of the limited area component of the system. Figure 1 shows the mean reduction of the analysis error in the steering flow for the 2004 typhoon season. Here, the error in the steering flow analysis is defined by the mass-weighted average of the root-mean-square error in the wind analysis between the 850 hPa and 250 hPa pressure levels. For verification, we used the operational NCEP global analysis. The figure shows that while the 200 km resolution limited area analyses were much less accurate than the global analyses, the higher resolution limited area analyses clearly reduced the error in the steering flow analysis compared to the global system. The improvement is almost uniform in the extratropics, while in the tropics clear improvements tend to occur in the immediate surrounding of storms. The latter result suggests that the limited area analysis provides a better representation of the interactions between the circulation of the storm and the wind field in its immediate vicinity.

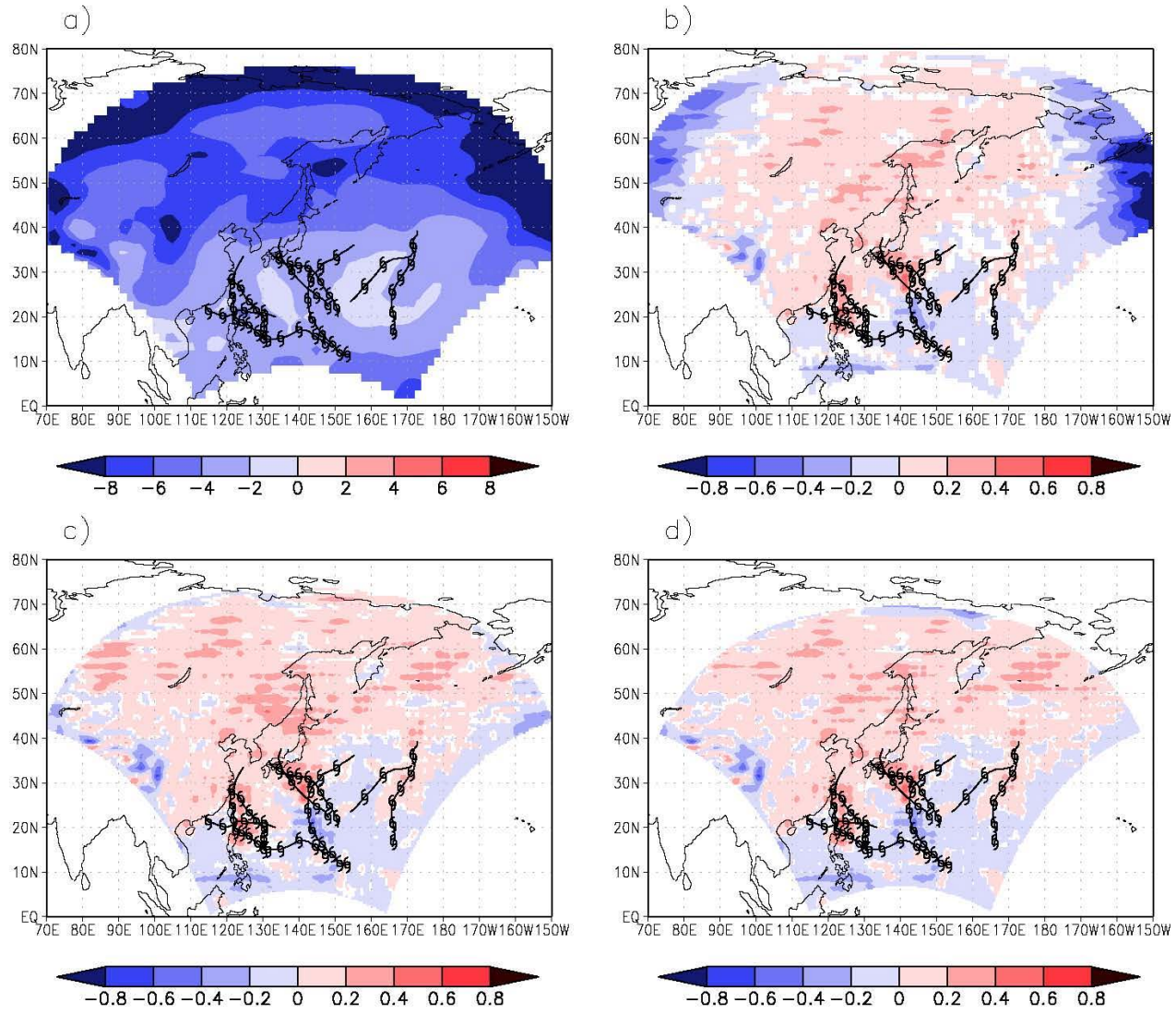

Figure 1. *Difference between the root-mean-square steering flow errors for the global analysis and the limited area analyses at horizontal resolutions of a) 200 km, b) 100 km, c) 48 km and d) 36 km. Positive values indicate superior limited area analysis performance. The tracks of the different typhoons are also indicated.*

Do these improvements occur because the limited area system improves the background, or because the higher resolution data assimilation system can more efficiently correct the background based on the information provided by the observations? (We recall that the background is the short-term forecast that the data assimilation updates to obtain the analysis.) To answer this question, we first show the root-mean-square error for the background in the different configurations of the data assimilation system (Fig. 2). Except for the 200 km resolution configuration, the background is more accurate in the limited area system. Next, we compare the magnitude of the reduction of the background error by data assimilation in the global and the limited area system (Fig. 3). The results show that the reduction in the background error is larger in the limited area system at all resolutions tested here.

While the resolution of our analysis/forecast systems is lower than that currently used in operations, we believe that our general conclusion, that the higher resolution of the limited area system improves the analysis due to both the improvement in the background and the more efficient correction of the background is likely to hold for most state-of-the art analysis/forecast systems. When the limited area model has advanced features other than a higher resolution, the limited area background may have a larger advantage over the global background; and the corrections in the background may also improve due the potentially more accurate estimates of the background error covariances.

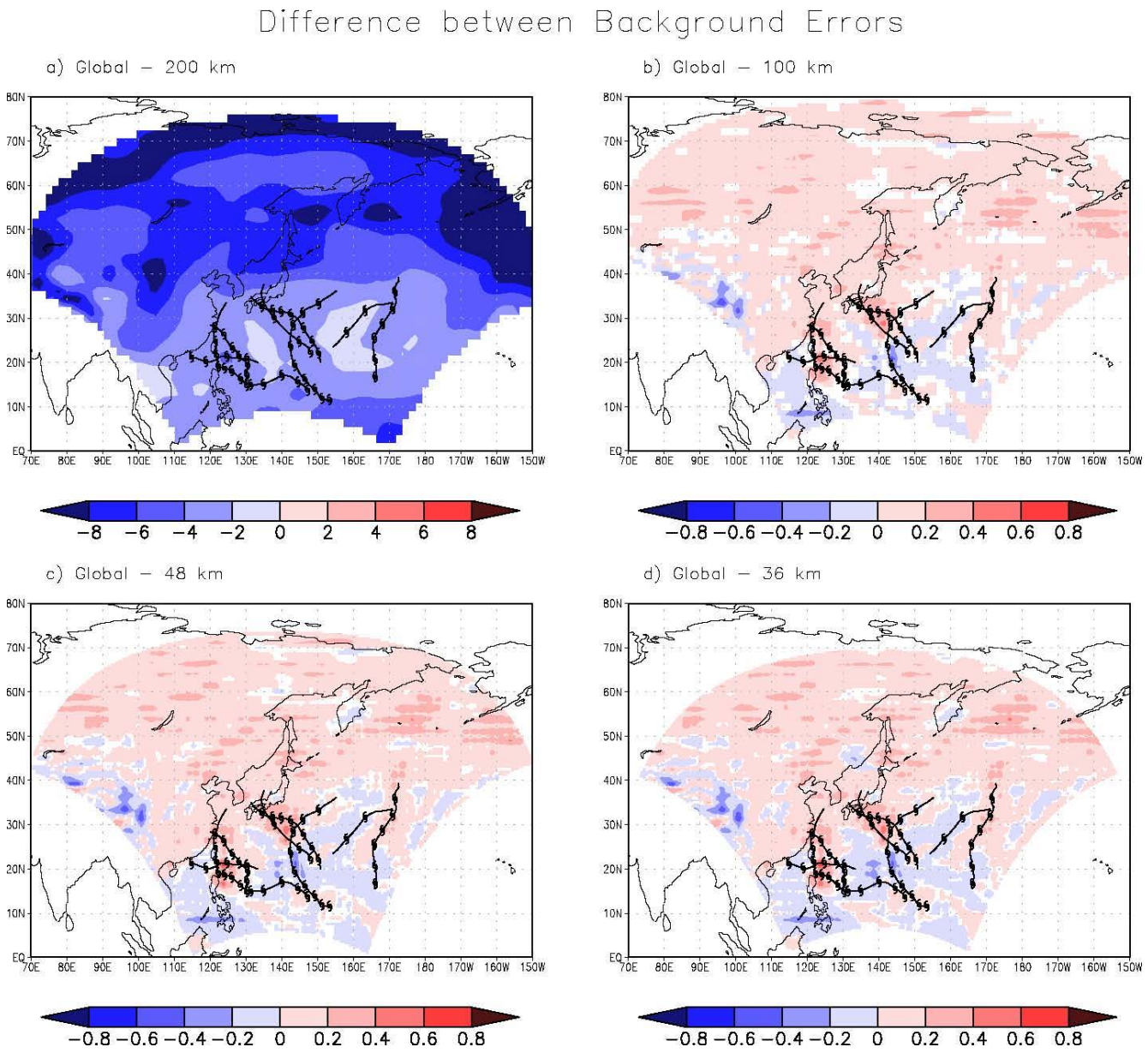

Figure 2. *Same as Fig. 1 except for the background error instead of the analysis error.*

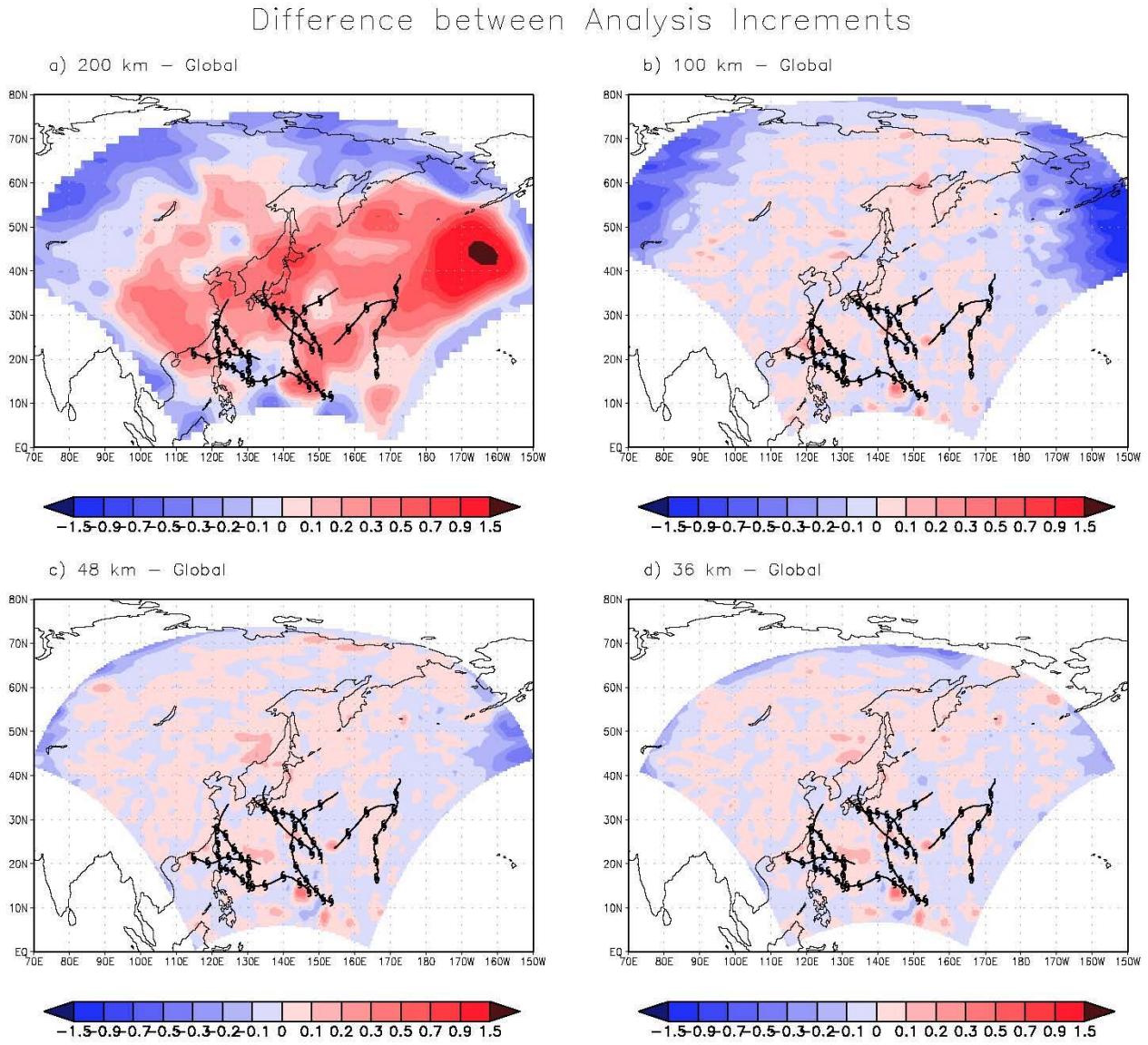

Figure 3. *The difference between the magnitudes of the background error reduction by the assimilation of observations in the global and the limited area analyses. Results are shown for the limited area analyses of a) 200 km, b) 100 km, c) 48 km, and d) 36 km resolution. Positive values indicate that the limited-area system reduced the background error more than the global system. The tracks of the different typhoons are also indicated.*

2008 Typhoon Season (TCS-08)

For the assimilation of the observations collected during the 2008 typhoon season, we used the same analysis/forecast system as for the assimilation of observations for 2004. The one important difference in the design of the experiments for the two different years is that for 2008 limited area calculations were carried out only at 48-km resolution. For 2008, we assimilated all observations collected in TCS-08 that made it to the operational data stream in real time, in addition to the routinely collected

observations. In general, the errors in the position of the typhoons are smaller for the 2008 than the 2004 season. Since we used the same systems for both years, we attribute the improvement of the performance of the system to the availability of extra observations collected in TCS-08.

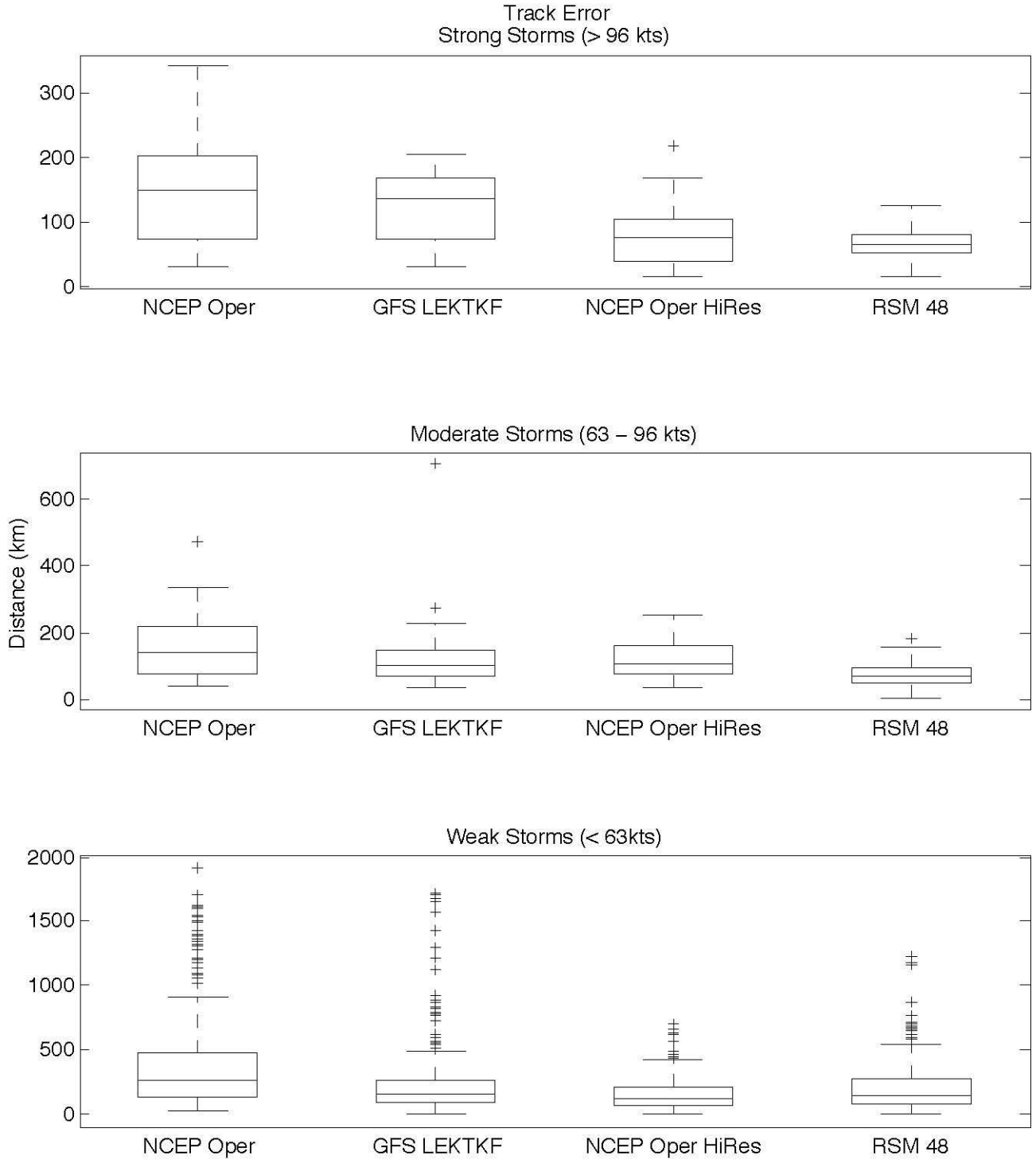

Figure 4. *Stratification of the distribution of the position analysis errors by storm intensity. The distributions are obtained by grouping errors for all Category 3 and 4 cyclones (top), Category 1 and 2 cyclones (middle), and tropical storms and depressions (bottom). The computation of the position error is based on JTWC Best Track data.*

The most notable result is that for strong and moderate (Category 1-5) storms, our limited area analysis performs better in terms of the accuracy of the position analysis than the high-resolution operational NCEP system (Fig. 4). (In Fig. 4, "NCEP Oper" and "NCEP Oper HiRes" are both based on the operational global analysis, but for "NCEP Oper" the verification is done on a 2.5^{o} resolution grid, while for "NCEP Oper HiRes" the verification is done on a 1^{o} resolution grid.) What makes this result particularly interesting is that for the 2004 season our limited area system did not perform better than the high-resolution operational NCEP system. Considering that NCEP made several major updates to their operational system between 2004 and 2008, including increasing the resolution to T382 (about 33 km at 20^{o}N) from T254 (about 50-km resolution), while our system was unchanged, we conclude that our system made a more efficient use of the available extra observations from TCS-08. There are two potential factors that may contribute to this result: (1) NCEP assimilated a large number of radiance observations, thus the added observations may provide a more limited amount of information about the atmospheric state; (2) NCEP uses a cyclone relocation algorithm (Rogers 2009) to enhance the position analysis based on TCVitals (2007), while our system prepares the analysis solely based on the assimilated observations. Thus the value of the added observations available for assimilation is higher for our system.

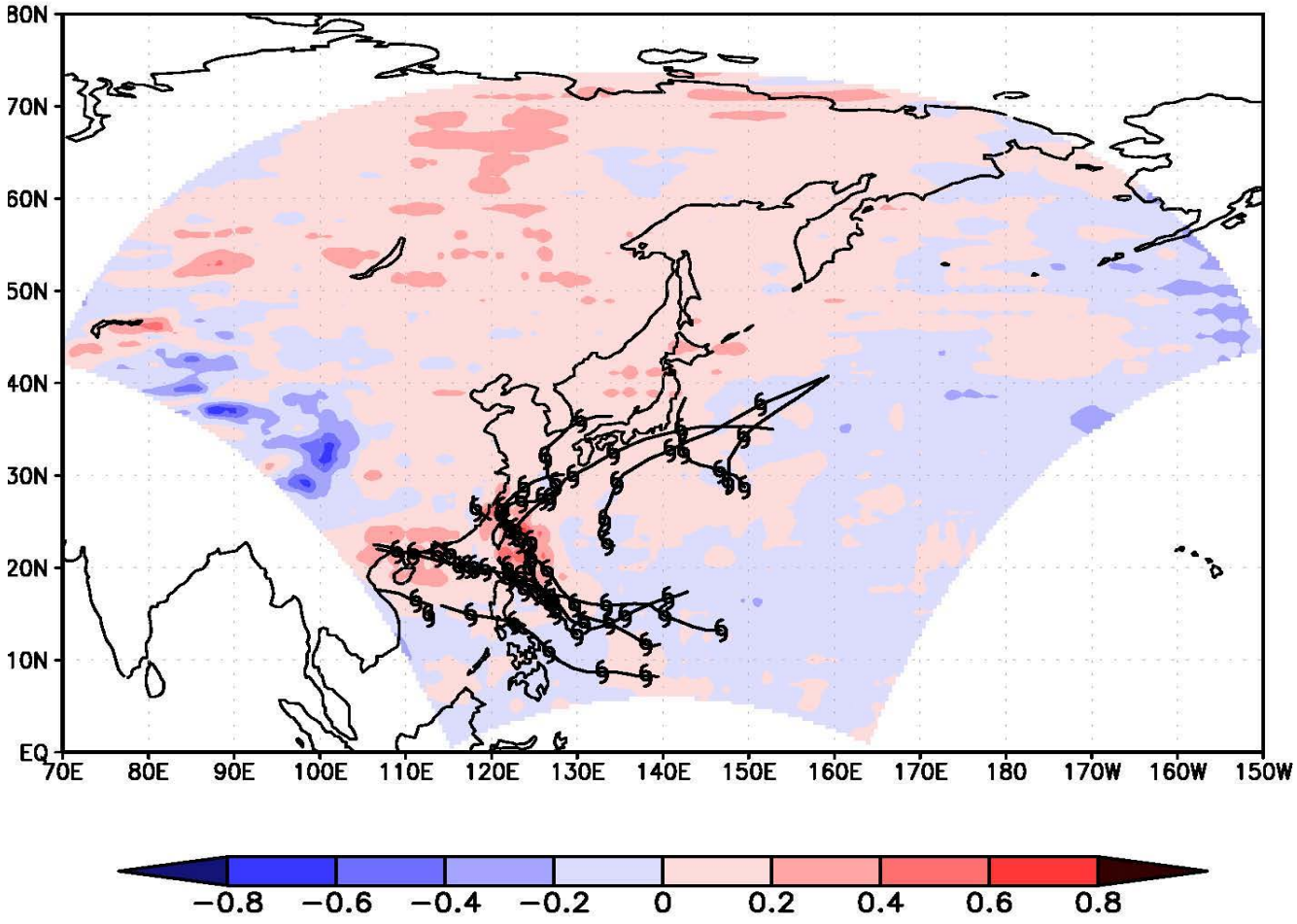

Figure 5. *Same as Fig. 1.c, except for the 2008 season.*

We suspect that the better performance of the operational system in locating weak storms is due to its use of TC relocation.

For a direct comparison of the results for the 2004 and 2008 seasons, we also show the mean error in the steering flow analysis for 2008 (Fig. 5). While the results are qualitatively very similar to those for the 2004 season, the improvements in the immediate surrounding of the storms are larger for the 2008 season, which we attribute to the availability of extra observations at those locations.

Assimilation of QuikSCAT Observations[1]

This project component makes use of ultra-high resolution (UHR) scatterometer winds. Professor David Long at Brigham Young University has generated the UHR scatterometer winds by resampling Level 1B QuikSCAT scatterometer data ("slice" data; Early and Long, 2001; Long et al., 2003). The scatterometer indirectly measures ocean surface roughness from the backscatter of radar pulses on the sea surface. A pulse illuminates an area that is roughly elliptical and approximately 25x37 km. Range and Doppler binning of a pulse measurement on board QuikSCAT divides a pulse into 8-12, non-overlapping "slices", parallel to the pulse minor axis, with Doppler range extending along the pulse major axis. The slices are each roughly $6 \cdot 25$ km. Because of QuikSCAT's rotating measurement geometry using two pencil beams, the satellite's 1800 km-wide swath is covered by overlapping pulse measurements of the sea surface from many different azimuth and at two elevation angles relative to the satellite. It is the diversity of pulse viewing geometries and polarizations from multiple measurements over the same patch of the sea that gives QuikSCAT its ability to estimate wind direction. The overlapping observations also allow the BYU image enhancement that uses image reconstruction techniques.

To produce QuikSCAT winds at a nominal resolution of 25 km (i.e., Level 2B processing), the slices from a single pulse with centroids within a single Wind Vector Cell (WVC) are joined to create that part of the whole pulse "egg" that is assigned to the WVC. WVCs are a grid of square cells across and along the satellite measurement swath. The set of (partial) pulse eggs associated with any given WVC is used to retrieve an estimate of the wind speed and direction at the centroid of the eggs within that WVC. To produce 12.5 km QuikSCAT winds, the pulse slices are assigned to 12.5 km WVCs before wind retrieval. Similarly, for the ultra-high resolution QuikSCAT winds, pulse slices are binned spatially into a 2.5 km WVC grid. The number of pulses contributing to WVCs, whether pulse eggs or pulse slices, decreases with higher resolution. That is, 25 km WVCs contain samples from many more pulses than the comparitively small 2.5 km WVCs. With less information (i.e., fewer samples), the higher resolution QuikSCAT winds become more noisy. Plagge et al. (2008) show in their study of ultra-high resolution QuikSCAT winds in the Gulf of Maine that the RMS of wind speed and direction is 2.3 m/s and 50 degrees, compared to 2.0 m/s and 20 degrees for the nominal 25 km QuikSCAT winds.

[1] This part of the report is based on the annual report submitted to Texas A&M by AER Inc.

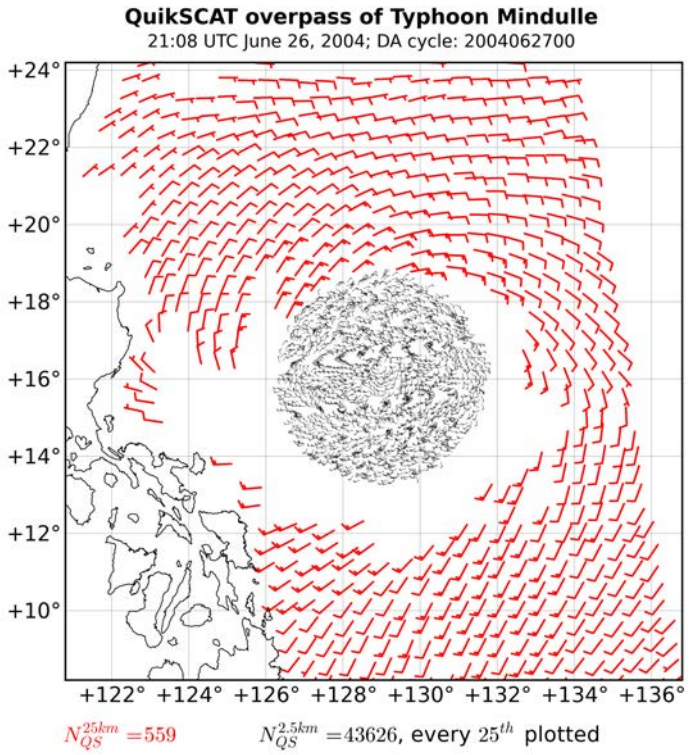

Figure 6. *Scatterometer winds around Typhoon Mindulle, valid at approximately 21:08 UTC, June 26, 2004. The red wind barbs are 25 km QuikSCAT winds (full barb 10 m/s, small barb 5 m/s) while the small black barbs are the 2.5 km ultra-high resolution (UHR) winds, thinned for plotting to every 25th observation.*

QuikSCAT quality control

Rain contamination is the most common quality issue for scatterometer winds (Hoffman and Leidner, 2005) and particularly for this study that focuses on tropical cyclones. In low wind conditions, rain increases the measured backscatter from both a rain-roughened sea surface and volume backscattering by the rain drops resulting in artifically higher winds. In high wind conditions (e.g., near the center of tropical cyclones), rain decreases the backscatter signal, because volume backscattering from the rain is not as strong as the backscatter from a very rough sea surface. Volume backscatter can also partially or totally depolarize the microwave backscatter wiping out some of the scatterometer's ability to determine to wind direction.

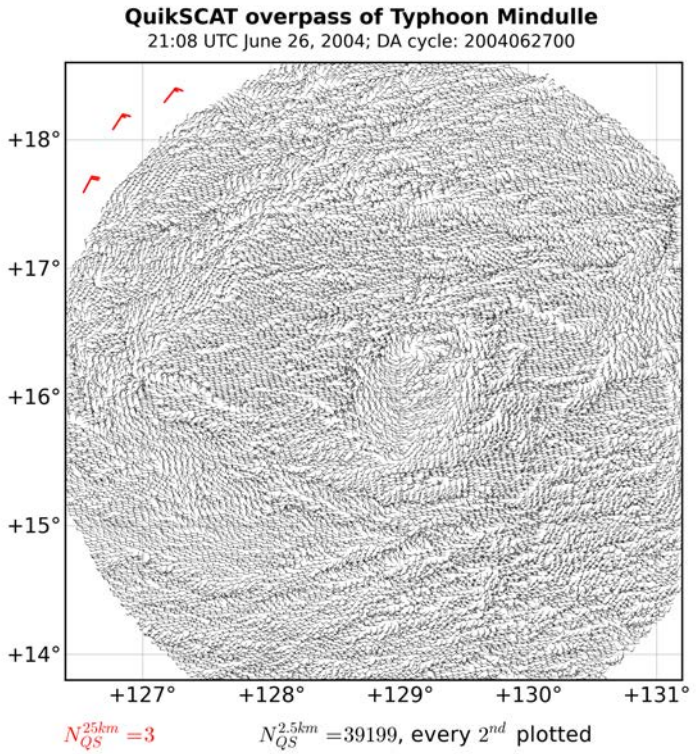

Figure 7. *Smaller region of the scatterometer winds around Typhoon Mindulle shown in Fig. 1 to highlight the ultra-high resolution (UHR) winds. Same plotting convention as Fig. 6, except the UHR scatterometer winds are thinned for plotting to every other observation.*

A great deal of effort has been expended by the science community to flag rain contaminated scatterometer winds or perhaps account for the effect of rain on retrieved scatterometer winds. The 25 km QuikSCAT winds used in this study have been preprocessed by NCEP and include NCEP quality marks. NCEP observation preprocessing removes all 25 km winds that are rain-flagged and excludes all winds in the "outer swath". Rain-contamination typically effects winds within 100-300 km of the center of tropical cyclones, the very region with the highest winds, wind speed gradients and important asymmetries in the wind field. Figure 6 shows an example of 25 km QuikSCAT rain-free winds around Typhoon Mindulle (2004). See the figure caption for more details. Notice that scatterometer winds are missing entirely for some distance from the approximate center of circulation. These winds are marked as rain-contaminated in the Level 2B data and are withheld from any subsequent processing or analysis by being assigned failing NCEP quality marks.

The UHR winds are experimental and do not contain a rain flag or any quality indicators. Owen and Long (2011) produced UHR winds using a joint wind/rain retrieval for selected cases that showed improvement in the retrieved winds under rainy conditions. But this method was not used to process the entire QuikSCAT mission. In this study, we use quality information concerning the impact of rain from a 12.5 km product that uses a joint wind/rain retrieval (Stiles and Dunbar, 2010). UHR and 12.5 km scatterometer winds were obtained for Typhoons Mindulle (2004) and Sinlaku (2008) from BYU (http://www.scp.byu.edu/data/Quikscat/HRStorms/HRStorm_DB.html) and the JPL PO.DAAC (http://podaac.jpl.nasa.gov/datasetlist?search=QUIKSCAT), respectively.

Data preparation for the high resolution winds for LETKF

Existing preprocessing software to convert NCEP PREPBUFR files to LETKF observation input format was modified to incorporate the UHR winds. Initially, UHR winds were added to the LETKF input observation file within a manually-specified radius of the cyclone best track position closest in time to the satellite overpass (Fig. 6, black wind barbs). But rain contamination of the UHR winds and the very high spatial resolution of the observations (2.5 km) compared to the analysis (48 km) have lead us to explore an approach that produces "super obs" at 25 km or 12.5 km resolution by averaging the UHR winds that are quality controlled with information from corresponding 12.5 km wind/rain retrievals. This work is part of future enhancements. Data sets were made for various time periods during Mindulle (2004) and Sinlaku (2008) for testing the preprocessing and LETKF codes, and evaluation of the impact of the assimilation of single observations and full scatterometer data sets.

Design and implemention of a new scatterometer observation function

The RSM as implemented for this project does not have a computational level at the height of scatterometer observations (10 meters above the sea surface), so a new scatterometer observation function was implemented in LETKF to compute the model-equivalent background wind at 10 m. The approach assumes that the boundary layer is well mixed, so virtual potential temperature should be constant with height from the surface through the boundary layer. The approach also assumes neutral thermodynamic stability in the model boundary layer, since the retrieved QuikSCAT winds are neutral-stability winds. The assumption of neutral stability for this study is appropriate given the amount of vertical mixing induced by the wind field around tropical cyclones. The RSM configuration uses 28 sigma model levels from the surface to the model top, with the lowest model level at about 42 meters above ground level. Details of the calculation of the model-equivalent, 10 meter background wind are given below.

Given the definitions of potential temperature and virtual potential temperature,

$$\theta = T/X \quad \text{and} \quad \theta_v = \theta(1+0.61w), \quad \text{where } 1/X = (p_0/p)^{(R/cp)}$$

compute θ, and then θ_v, at the lowest model sigma level. Since θ_v and w are constant with height in a well-mixed boundary layer, we solve for mean sigma layer density, $\underline{\rho}$, using the average layer pressure, $\underline{p}=(p_{sfc}-p_1)/2$,

$$\theta_v = \theta(1+0.61w)$$

$$\theta_v = (\underline{T}/\underline{X})\,(1+0.61w), \quad \text{where } 1/\underline{X} = (p_0/\underline{p})^{(R/cp)}$$

We remove dependency on $\underline{T}$ by substituting in from the equation of state, $\underline{T}= \underline{p}/(\underline{\rho}R)$, and solve for mean density:

$$\theta_v = \underline{p}/(\underline{\rho}R\underline{X})\,(1+0.61w)$$
$$\underline{\rho} = \underline{p}/(\theta_v R\underline{X})\,(1+0.61w)$$

Then given the mean density of the lowest sigma layer (from the last equation), we compute the height of the first sigma layer (dz in meters) and the pressure at 10 meters (dp in Pa) via the hydrostatic equation,

$$dp/dz = -\underline{\rho}g$$

While $\underline{\rho}$ is not an exact calculation of density at 10 meters, it does provide a very reasonable estimate for the purpose of estimating the pressure at 10 meters.

Knowing the height of the lowest model sigma layer, z_1, allows for the use of an empirical relation to estimate z_0, the surface roughness height, assuming neutral stability (Hoffman, 2011; eqn 12). And knowing the surface roughness height, z_0, the lowest sigma layer wind can be reduced to a 10 meter wind using the log wind relation:

$$V_{10} = V((\log_{10}(10.0/z_0)) / (\log_{10}(z_1/z_0))$$

Single observation tests

To verify the new scatterometer observation function, single observation tests were performed comparing the result of assimilation at the lowest sigma level. The single observation tests also helped determine an appropriate vertical extent of influence for scatterometer data. As expected, the coherent spatial structure of tropical cyclones in the vertical resulted in meaningful correlations throughout the depth of the troposphere. The vertical window of influence used in the single observation experiment reported below is 0.35 times the local scale height of the atmosphere. The single obs experiment background ensemble is from the standard experiment for Typhoon Mindulle valid at 00 UTC 27 June 2004. The observations used at this time from QuikSCAT are valid at 2108 UTC 26 June and Mindulle is located at about 16N, 130E. For the example shown in the accompanying figures, the single obs is located due east of the typhoon center at 16.31N, 132.78E and has wind components of (u,v) = (-3.9, 14.4) m/s. This corresponds to O-B increments of (3.5, 6.9) m/s. The assigned observation standard deviation is 2 m/s, and the ensemble background standard deviation is (1.34, 1.16) m/s. LETKF uses a 800 km horizontal localization radius (with a taper beginning at 500 km). These tests were performed on a 48 km-resolution RSM, limited-area domain, and the winds were assimilated at either k=1 (the lowest sigma level) or at 10 meters using the new observation function. Figure 9 shows the analysis increments (A-B) in map view at the lowest sigma level but using the new observation function. Note the large asymmetry of the increments relative to the observation location due to the ensemble correlations. Figure 9 shows a vertical profile along the east-west line through the observation. The largest increments (A-B, top) are not at the surface but at about the 5th sigma level. The apparent secondary maximum at the 9th sigma level is due to vertical localization and the contouring algorithm. The bottom panel shows the difference between the experiments with the new observation operator and the simple assignment of the observation at the lowest model level. The differences are small but introduce a bias. By assigning the 10 m wind to a higher level, the observation will be biased low in the original scheme. The new obs operator corrects this and the analyses with the new operator will have higher wind speeds.

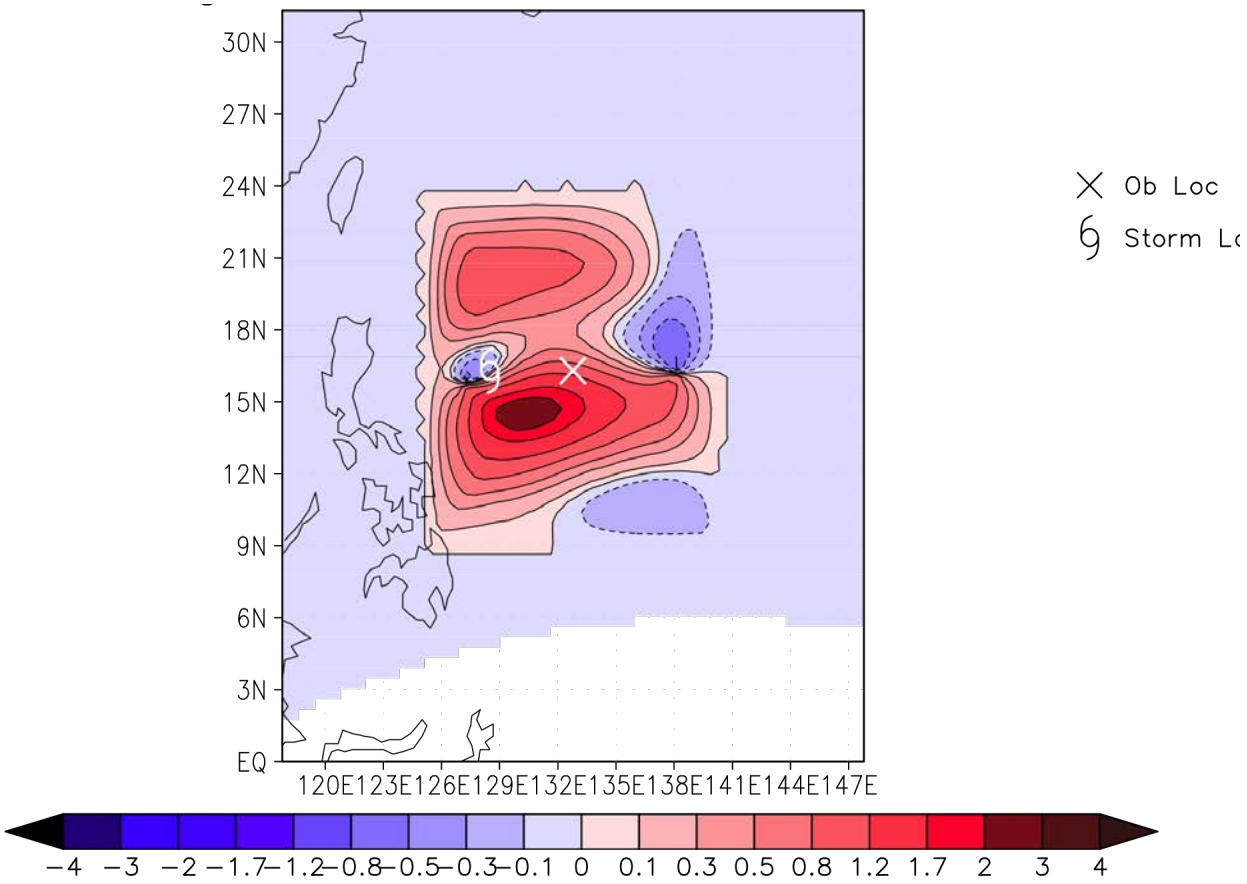

Figure 8. *Single obs experiment showing the analysis increments at the lowest model level (k=1) for wind speed for the case where the wind observation is assimilated at 10 m using the new observation function.*

The strong vertical correlations found by LETKF between the surface and the top of the vertical window of influence in these results (cf. top panel of Fig. 9 at sigma level 7500) suggest that the scatterometer data should be allowed to influence higher levels in the troposphere. Through further single observation experiments, we increased the vertical window of influence to find if the correlations tail off to small values high in the troposphere. Near-zero correlcations high in the troposhpere might indicate a natural limit of vertical window of influence for these data. Figure 10 shows the analysis increments for the same single observation test described above, but using a vertical window of influence of 2.0 times the scale hight. Notice that meaningful vertical correlation is found by LETKF between the scatterometer observation and many points throughout the troposphere. This suggests that for assimilation near tropical cyclones that have coherent vertical strucuture throughout the troposphere, a vertical assimilation window of at least two times the scale height is appropriate.

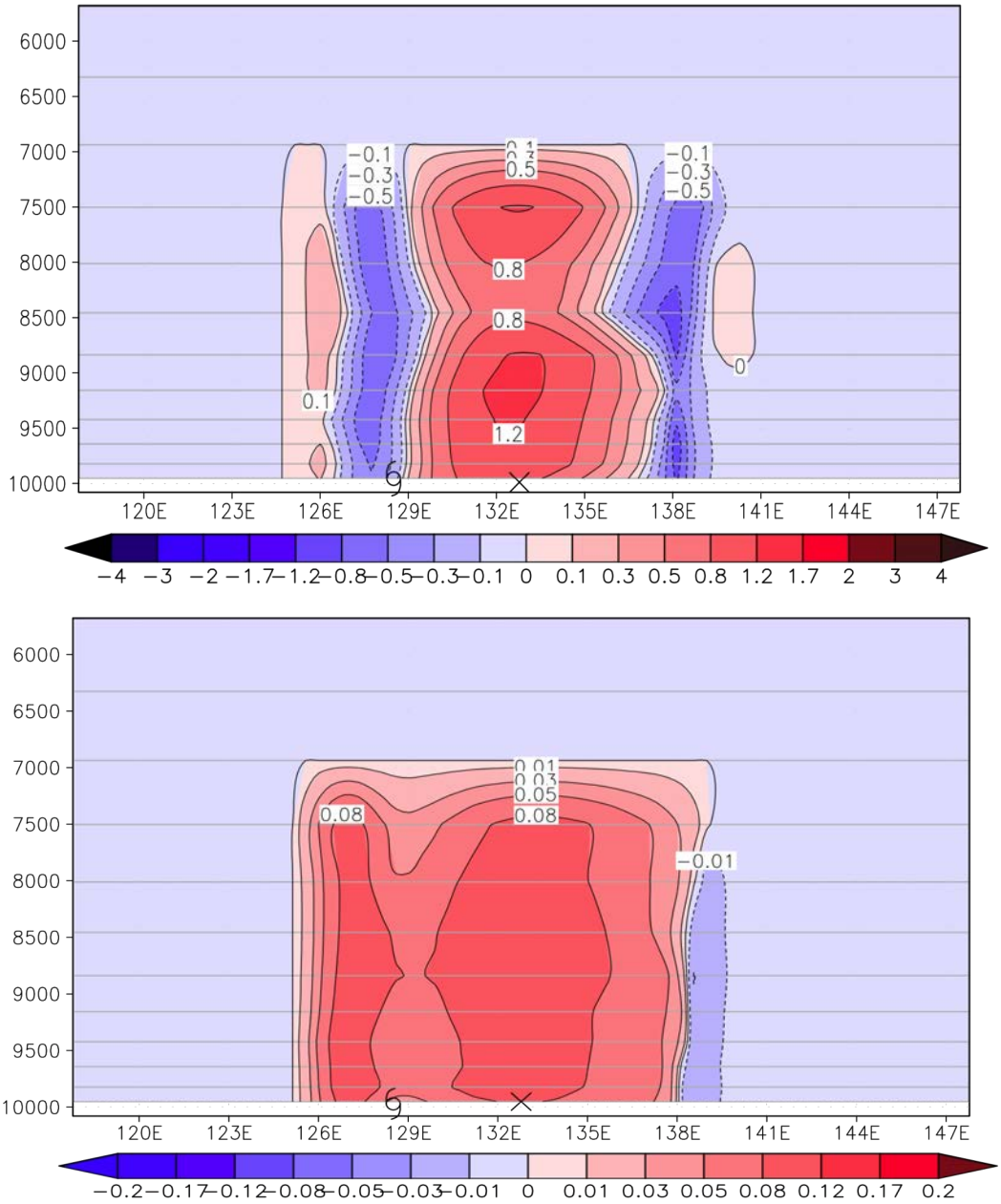

Figure 9. *Single obs experiment showing analysis increments in cross section for wind speed for the case where the wind observation is assimilated at 10 m using the new obs function (top) and the difference between this analysis and the analysis where the same wind observation is assimilated at the lowest model level (bottom). The vertical coordinate is model sigma level times 10,000. The horizontal gray lines are the model sigma levels.*

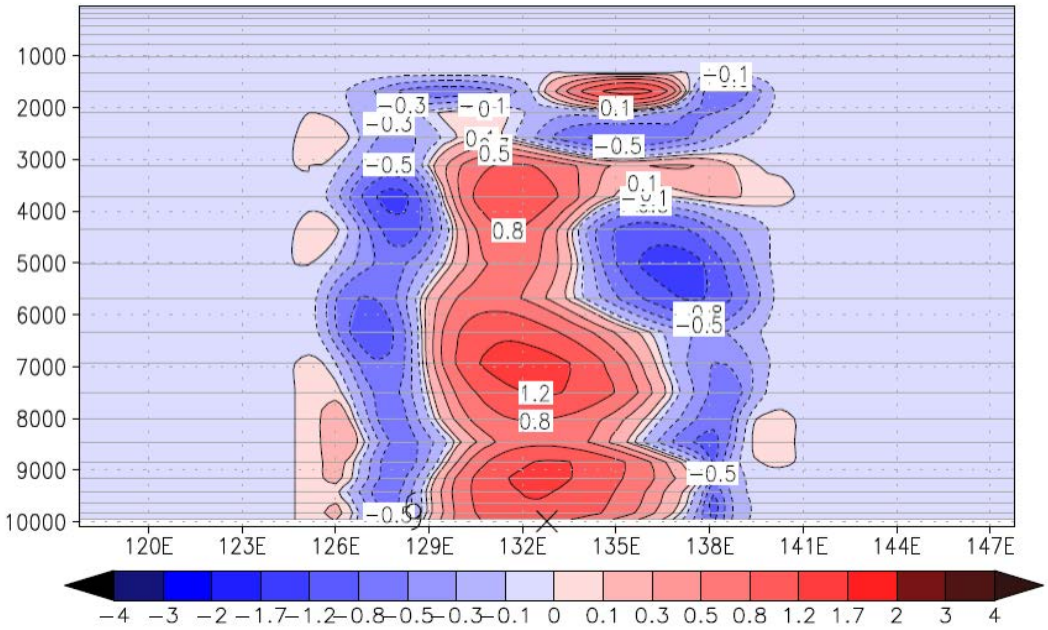

Figure 10. *Same as top panel of Fig. 9, but using a vertical localization of 2.0 times the scale height of the atmosphere.*

Joint-State Approach

The key aspect of the joint state approach is the definition of a cost function for the joint state of the global and the limited area model: the minimizer of this cost function provides the analyses for both systems. The two parameters introduced into the cost function by the joint state approach are (i) the parameter that controls the proper weighting of the global and the limited area state in the observation function and (ii) the weight of a penalty term that controls the differences allowed between the global and the limited area analyses in the region where they are both available. Our efforts this year were focused on investigating and documenting the sensitivity of the approach to the aforementioned two parameters. The results of this investigation are included in the paper Yoon et al. (2012).

IMPACT/APPLICATIONS

Our results add to the growing body of evidence that ensemble-based Kalman filters provide an efficient way of data assimilation in the presence of TCs. In particular, ensemble based Kalman filters do not require the use of “TC relocation” or “bogusing” approache which are still used in some variational data assimilation systems. The results also suggest that in order to realize the potentials of the ensemble based filter, it is important to have a good observational coverage around the TCs.
Our results also indicate that a coupled global-limited-area data assimilation system can take advantage of the higher resolution model information provided by the limited area component of the system in regions where TCs form and evolve.

The strategy for the coupling of the global and the limited area data assimilation componets can, most likely, be further improved. One candidate for such an approach is described by Yoon et al. (2012). We are in the process of extending our reseach efforts on that topic in close collaboration with researchers of the Naval Research Laboratory, Monterey. We hope that these efforts will eventually lead to an enhancement of the US Navy weather forecasting capability.

REFERENCES

Early, D. S. and D. G. Long, 2001: Image reconstruction and enhanced resolution imaging from irregular samples, *IEEE Transactions on Geoscience and Remote Sensing*, **39**, 291-302.

Hoffman, R. N. and S. M. Leidner, 2005:. An introduction to the near real-time SeaWinds data. *Wea. Forecasting*, **20**, 476-493.

Hoffman, R. N. and S. M. Leidner, 2010: Some characteristics of time interpolation errors for fluid flows. *J. Atmospheric Oceanic Technology*, **27**,1255–1262. doi:10.1175/2010JTECHA1429.1.

Hoffman, R. N., 2011: Neutral stability height correction for ocean winds, http://arxiv.org/pdf/1107.1416.pdf.

Hunt, B. R., E. J. Kostelich, and I. Szunyogh, 2007: Efficient data assimilation for spatiotemporal chaos: a Local Ensemble Transform Kalman Filter. *Physica D*, **230,** 112-126.

Keyser, D., 2007: Format of tropical cyclone vital records “TCVITALS”. Tech. Rep., NCEP Environmental Modeling Center. URL: http://www.emc.ncep.noaa.gov/mmb/data_processing/tcvitals_description.htm

Long, D. G., J. B. Luke and W. Plant, 2003: Ultra high resolution wind retrieval from SeaWinds, *Proceedings of IEEE International Geoscience and Remote Sensing Symposium*, **2**, 1264-1266.

Merkova, D., I. Szunyogh, and E. Ott, 2011: Strategies for coupling global and limited-area ensemble Kalman filter assimilation. *Nonlin. Processes Geophys.*, **18,** 415-430.

Ott, E. and co-authors, 2004: A local ensemble Kalman filter for atmospheric data assimilation.*Tellus*, **56A,** 415-428.

Owen, M. P., K. M. Stuart and D. G. Long, 2007: Ultra-high-resolution near-coastal wind retrieval for QuikSCAT, in Coastal Ocean Remote Sensing, Proceedings of SPIE, Vol. 6680, August 26-27.

Plagge, A. M., D. C. Vandemark and D. G. Long, 2009: Coastal validation of ultra-high resolution wind vector retrieval from QuikSCAT in the Gulf of Maine, *IEEE Geosci. Remote Sens. Lett.*, **6**, 413-417. doi:10.1109/LGRS.2009.2014852.

Rogers, E., et al., 2009: The NCEP North American mesoscale modeling system: Recent changes and future plans. Preprints, 23nd Conf. on Weather Analysis and Forecasting/19th Conf. on Numerical Weather Prediction, Omaha, NE [Available online at http://ams.confex.com/ams/pdfpapers/154114.pdf.], American Meteorological Society, 2A4.

Stiles, B.W. and R.S. Dunbar, 2010: A neural network technique for improving the accuracy of scatterometer winds in rainy conditions, *IEEE Transactions on Geoscience and Remote Sensing*, **48**, 3114-3122.

Szunyogh, I. and co-authors, 2008: Szunyogh, I., E. J. Kostelich, G. Gyarmati, E. Kalnay, B. R. Hunt, E. Ott, E. Satterfield, and J. A. Yorke, 2008: A Local Ensemble Transform Kalman Filter data assimilation system for the NCEP global model. *Tellus,* **60A,** 113-130.

Szunyogh I. and co-authors, 2005: Assessing a local ensemble Kalman filter: Perfect model experiments with the NCEP global model. *Tellus,* **57A,** 528-545.

Yoon, Y.-N., B. R. Hunt, E. Ott, and I. Szunyogh: Ensemble regional data assimilation using joint states. *Tellus.* (in press).

PUBLICATIONS

Holt, C. R., I. Szunyogh, and G. Gyarmati, 2012: Can a moderate resolution limited-area data assimilation system add value to the global analysis of tropical cyclones?. *Mon. Wea. Rev.* (under review).

Yoon, Y.-N., B. R. Hunt, E. Ott, and I. Szunyogh, 2012: Ensemble regional data assimilation using joint states. *Tellus.* (in press)

Holt, C. R., 2011: *Testing a coupled global-limited area data assimilation system using observations from the 2004 Pacific typhoon season.* Master of Science Thesis, Texas A&M University, 60 pp.

Merkova, D., I. Szunyogh, and E. Ott, 2011: Strategies for coupling global and limited-area ensemble Kalman filter assimilation. *Nonlin. Processes Geophys.*, **18,** 415-430.